



Influence of Waste Glass Powder as an Aluminosilicate Precursor in Synthesizing Ternary Blended Alkali-Activated Binder

P. Manikandan¹ · L. Natrayan² · S. Duraimurugan³ · V. Vasugi¹

Received: 2 August 2021 / Accepted: 5 November 2021 / Published online: 8 January 2022
© The Author(s), under exclusive licence to Springer Nature B.V. 2021

Abstract

The formation of alkali-activated binders from industrial end products and landfill materials attracts considerable interest in construction technology since it diminishes the waste products discarded into landfills. The impact of incorporating Waste Glass Powder (WGP) into Ground Granulated Blast Furnace Slag (GGBS) with Fly ash (FA) and Metakaolin (MK) on the workability and mechanical characteristics (Compressive, Split-Tensile, and Flexural strength) of a ternary blended geopolymer binders are investigated in this study. WGP was employed as the substitution for GGBS on the alkali-activated binder from 25 % to 40 % by total weight retaining the 10 % Fly ash and Metakaolin ratio. Sodium silicate solution and sodium hydroxide flakes were utilized in combination as the Reaction Generation Liquid (RGL). The fractions of sodium silicate solution to sodium hydroxide solution, RGL to binder ratio and the concentration of sodium hydroxide solution used in the study were considered as 2.5, 0.55 and 8 Molarity, respectively. The effect of varying combinations of WGP (25 % - 40 %) under ambient curing conditions on the workability and mechanical properties of the ternary mixture geopolymer binders were evaluated, and the optimum mix proportions were proposed. The maximum compressive (59.21 MPa), split-tensile (6.60 MPa), and flexural strength (5.70 MPa) results were obtained with a mixture of 55 % GGBS, 35 % WGP, and 10 % MK in an 8 M NaOH solution. The proposed work emphasizes the viability of incorporating optimum substitution levels of WGP (35 %) in developing sustainable ternary based geopolymer concrete by facilitating a long time resolution for the efficient exploitation of uninhibited glass wastes. The microstructural and mineralogical characterization of the geopolymer sample obtained using SEM-EDX and XRD techniques illustrated the presence of sodium aluminate silicate hydrate (N-A-S-H) gel and calcium aluminate silicate hydrate (C-A-S-H) gels as the end reaction product.

Keywords Geopolymer binder · Waste glass powder · Ground granulated blast furnace slag · Metakaolin · Fly ash · Reaction generation liquid

1 Introduction

Concerns regarding the ecological consequences of waste management have developed in response to the world's rapidly rising population and associated industrialization. Many industries are already developing waste recycling administration systems to comply with local and global

regulations. To reduce the adverse ecological consequences and safeguard natural raw materials, possible waste products are encouraged to be re-used and reproduced as primary or secondary source materials in any industrial process [1, 2]. The utilization of industrial by-products and recycled materials in construction and building materials for concrete work particularly inspires to minimize solid waste management and natural raw materials use [3–7].

Various academics have extensively researched waste glass as an alternative or partial substituting cement material and recycled aggregate in concrete [1, 8, 9]. WGP derived from broken glass panels and crushed containers exhibit pozzolanic reactivity; incorporating 10 % - 20 % of WGP as supplementary cementitious material in ordinary Portland cement (OPC) based concrete enhances compressive strength and improves later age strength to a considerable

✉ V. Vasugi
vasugi.v@vit.ac.in

¹ School of Civil Engineering, Vellore Institute of Technology, Chennai Campus, Chennai, India

² Department of Mechanical Engineering, Saveetha School of Engineering, SIMATS, Chennai, India

³ Fosroc Chemicals India Private Limited, Chennai, India

extent [8]. Kou and Poon evaluated the impact of fine aggregate generated from recycled glass cullet on the workability and mechanical characteristics of self-compacting concrete (SCC). Their experimental findings revealed greater workability and decreased mechanical properties as the glass cullet proportion increased [9]. Meantime, increasing the WGP level in the OPC-based concrete minimized the drying shrinkage and enhanced the resistance against chloride ion penetration [10]. In architectural mortar mixes, the composition of 20% substitution levels of WGP in white-based OPC and 100% replacement of waste glass cullet as fine aggregate produces significant compressive strength results [11]. On the other hand, increment of the WGP substitution levels in cement concrete beyond a certain proportion (greater than 15%) results in the gradual decrease in mechanical performance, cracking effects and expansion because of the emergence of alkali-silica reaction among the silica constituents in WGP and aluminum components in cement materials [12, 13].

Geopolymer is a new substitute cementitious substance produced as the reaction product from geopolymerization of aluminosilicate or geopolymeric source materials activated by Reaction Generation Liquid (RGL) [14–16]. A characteristic RGL comprises the amalgamation of either sodium silicate + sodium hydroxide (or) potassium silicate + potassium hydroxide solution. Any aluminosilicate source material with an adequate amount of aluminum and silicon content derived from industrial by-products, geological sources, or recycled waste can be used for geopolymer concrete preparation [17]. Compared to OPC-based concrete, alkali-activated binders possess exceptional mechanical strength characteristics [18], fire resistance [19], durability properties [20] and chemical attack [21] influenced by the kind of aluminosilicate precursors employed. The most extensively consumed aluminosilicate source materials in the production of alkali-activated concrete are GGBS and Fly ash [12, 22]. In addition, various research articles have suggested that industrial by-products and waste materials like rice husk ash [23], silica fume [24], sawdust [25], municipal solid waste incinerated ash [26], waste glass powder [27], and Metakaolin [28] might be employed to supplement either GGBS or Fly ash for geopolymer matrix production. The preparation of geopolymer binders from various aluminosilicate source materials is exploring practical applications in the construction of roadways, precast structural elements, railway sleepers, highway crash barriers, sewer pipelines, pavement blocks, mortar for repair works, etc. [29, 30].

Until now, investigations on the effective utilization of WGP in alkali-activated Fly ash/GGBS based binders are scarce to our best knowledge. Moreover, the literary works on the prospective incorporation of WGP in ternary blended geopolymer preparation are minimal. Hence, this research article attempted to evaluate the possibility of utilizing

WGP as a potential geopolymeric source activator to prepare a ternary blended geopolymer matrix with GGBS and Metakaolin/Fly ash. The workability and the mechanical performance (compressive strength, split-tensile strength, and flexural strength) of the geopolymer samples were estimated, and the optimum replacement percentage of WGP in ternary geopolymer concrete is proposed. Further, the mineralogical and microstructural investigations are carried out on the geopolymer specimen yielding maximum mechanical strength characteristics using X-ray diffraction (XRD), scanning electron microscopy (SEM) and energy-dispersive X-ray spectroscopy (EDX) analysis.

2 Materials and Experimental Approach

2.1 Materials

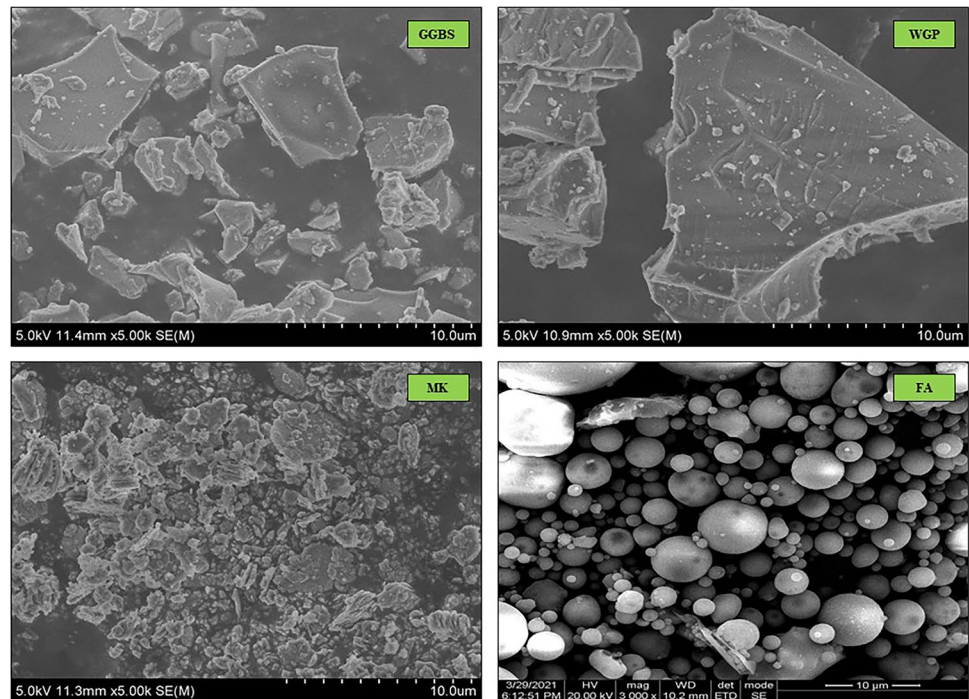
The precursor materials employed in this study to produce geopolymer binder include GGBS, WGP, Metakaolin, and Fly ash. The WGP is procured by crushing the broken glass panels in the ball mill for 60 min to obtain a particle size lesser than 75 microns. GGBS and low calcium Fly ash utilized in this study are sourced from JSW cements and North Chennai Thermal Power plant, Chennai, respectively. The Metakaolin used in this study is obtained from ASTRRA chemicals, Chennai. The chemical composition of the aluminosilicate source materials employed in this study is expressed in Table 1 using X-ray fluorescence (XRF) analysis.

Figure 1 displays the Scanning Electron Microscopy (SEM) images of the aluminosilicate precursor materials (GGBS, WGP, MK, and FA) used in the study to prepare a ternary-based geopolymer matrix. The SEM micrographs indicate that FA's morphology is primarily spherical, whereas MK is angular and platy in nature. In WGP and GGBS, the morphology of the particles is angular and irregular in shape. The X-ray diffraction (XRD) spectra of the aluminosilicate source materials are illustrated in Fig. 2. As seen in Fig. 2, it can be noted that crystalline components like Quartz (SiO_2), Calcite (CaCO_3) & Alumina (Al_2O_3) are present in GGBS, Quartz (SiO_2) & Cristobalite in MK, Quartz (SiO_2) & Mullite ($\text{Al}_6\text{Si}_2\text{O}_{13}$) in FA and WGP comprises highly amorphous phase.

Regionally available Manufacturing (M) sand with a specific gravity of 2.72, water absorption 3.15%, passing through 4.75 mm IS sieve confirming to Zone II according to IS: 383-1970 [31] with fineness modulus of 3.37 is utilized as the fine aggregates. The pulverized granite stone of size 20 mm obtained from a local quarry with water absorption of 0.50% and specific gravity of 2.63 is employed as coarse aggregates in the study. Commercially accessible NaOH flakes and sodium silicate solution sourced from ASTRRA

Table 1 Chemical constituents of aluminosilicate source materials

| | Identification | WGP | GGBS | Fly ash | Metakaolin |
|--------------------------|--------------------------------|-------|-------|---------|------------|
| Chemical composition (%) | SiO ₂ | 85.44 | 37.23 | 63.40 | 48.77 |
| | Al ₂ O ₃ | 2.40 | 14.42 | 26.82 | 43.33 |
| | CaO | 10.52 | 36.75 | 2.51 | 5.20 |
| | Fe ₂ O ₃ | 0.35 | 0.50 | 5.56 | 1.10 |
| | MgO | 0.12 | 8.39 | 0.40 | 0.24 |
| | ZnO | 0.01 | 0.02 | - | - |
| | TiO ₂ | 0.02 | 0.35 | - | 0.20 |
| | MnO | 0.03 | 0.10 | 0.01 | 0.02 |
| | Cr ₂ O ₃ | 0.08 | 0.03 | - | 0.01 |
| | LOI | 0.21 | 0.31 | 0.97 | 0.35 |
| Physical properties | Specific gravity | 2.55 | 2.62 | 2.16 | 2.50 |

Fig. 1 SEM micrographs of precursor materials

Chemicals, Chennai, are employed as the Alkali Activator solution in the study.

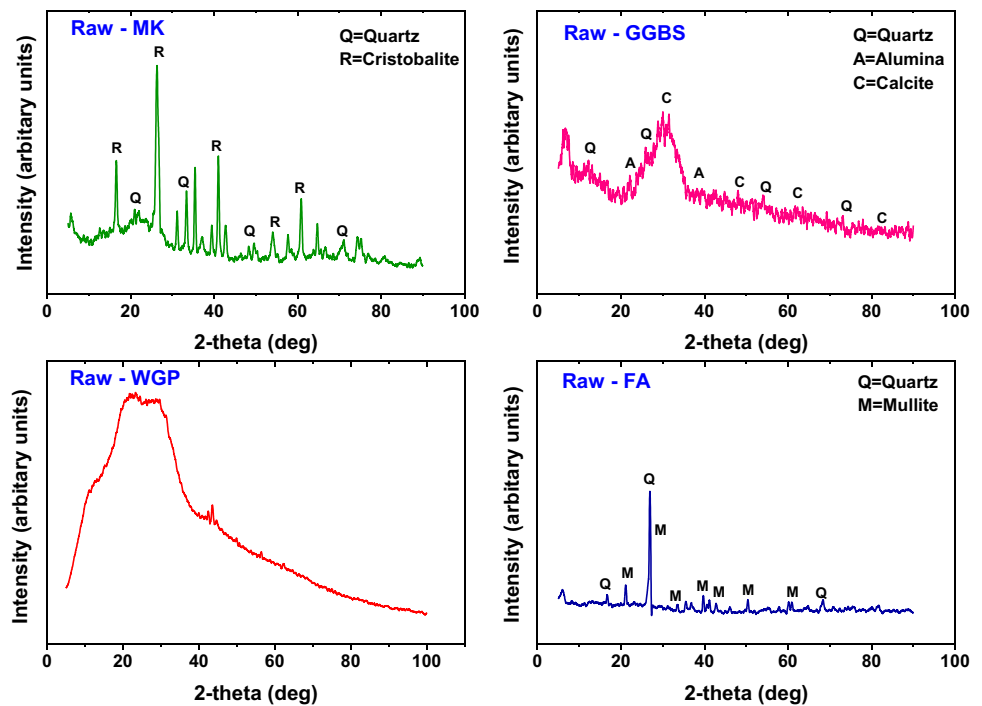
2.2 Experimental Approach

In this study, eight mix ratios are formulated to evaluate the replacement levels of WGP varying from (25–40%) in GGBS with a constant proportion (10%) of Fly ash and Metakaolin on the workability and mechanical properties of ternary geopolymer concrete under ambient curing environment. When GGBS is used as a precursor material in the synthesis of geopolymers, it generates a certain amount of heat during the polymerization reaction, eliminating the need for heat curing. The primary objective of this research is to assess the potential utilization of WGP as a GGBS

substitution in ternary blended geopolymer concrete. Generally, WGP encompasses a higher fraction of amorphous SiO₂ and fewer Al₂O₃; hence addition alumina is added to the system by incorporating 10% of MK/FA. Furthermore, preliminary test results revealed that introducing MK/FA source materials in ternary geopolymer systems greater than 10% does not provide adequate compressive strength, so the proportion of MK and FA has been established as 10% in this study.

The ratio of sodium silicate to sodium hydroxide, alkaline to the binder, and concentration of NaOH solution was maintained as 2.5, 0.55 and 8 M, respectively, for all the mix details. Auromix 500 (superplasticizer) procured from FOS-ROC Chemicals Private Limited, Chennai, obtains desired workability in the geopolymer matrix. The quantities of

Fig. 2 XRD patterns of aluminosilicate source materials



fine aggregates, coarse aggregates, sodium hydroxide, and sodium silicate adopted for all the mix ratios are 720 Kg/m^3 , 1080 Kg/m^3 , 60.82 Kg/m^3 and 152.08 kg/m^3 , respectively. The particulars of the mix proportions used in this study are illustrated in Table 2.

The workability characteristics of the geopolymer concrete are evaluated by conducting a slump cone test on the freshly prepared geopolymer concrete mix in accordance with IS-7320 provisions [32]. In addition, the compressive, split tensile and flexural strength characteristics of ternary blended geopolymer matrix were evaluated according to IS:516-1959 standards [33]. The compressive strength, split tensile and flexural properties were computed by testing geopolymer cubes of size $150 \times 150 \times 150 \text{ mm}$, cylinders of size $200 \times 100 \text{ mm}$ and prism samples of dimensions $500 \times 100 \times 100 \text{ mm}$, respectively. The

X-ray diffraction (XRD) technique is adopted to examine the crystallographic features of the aluminosilicate raw materials and geopolymer sample with the application of power diffraction file (PDF). The XRD technique provides a diffractogram pattern that indicates whether the sample is crystalline or amorphous or partially crystalline. The aluminosilicate precursors and geopolymer samples can be characterized microstructurally and elementally using field emission electron microscope and energy dispersive spectroscopy. For aluminosilicate raw materials and geopolymer specimens, SEM images at $10 \mu\text{m}$, 20 and $50 \mu\text{m}$ magnification are obtained. Further, the chemical characteristics, mineralogical constituents, and microstructural investigations are evaluated on the geopolymer sample producing maximum mechanical strength properties using EDX, XRD, and SEM analysis.

Table 2 Mix proportions of the ternary geopolymer concrete

| Mix No. | GGBS (Kg/m^3) | WGP (Kg/m^3) | MK (Kg/m^3) | FA (Kg/m^3) | Slag (%) | WGP (%) | MK (%) | FA (%) |
|---------|--------------------------|-------------------------|------------------------|------------------------|----------|---------|--------|--------|
| T1 | 251.60 | 96.78 | 38.70 | - | 65 | 25 | 10 | - |
| T2 | 232.25 | 116.13 | 38.70 | - | 60 | 30 | 10 | - |
| T3 | 212.90 | 135.48 | 38.70 | - | 55 | 35 | 10 | - |
| T4 | 193.54 | 154.84 | 38.70 | - | 50 | 40 | 10 | - |
| T5 | 251.60 | 96.78 | - | 38.70 | 65 | 25 | - | 10 |
| T6 | 232.25 | 116.13 | - | 38.70 | 60 | 30 | - | 10 |
| T7 | 212.90 | 135.48 | - | 38.70 | 55 | 35 | - | 10 |
| T8 | 193.54 | 154.84 | - | 38.70 | 50 | 40 | - | 10 |

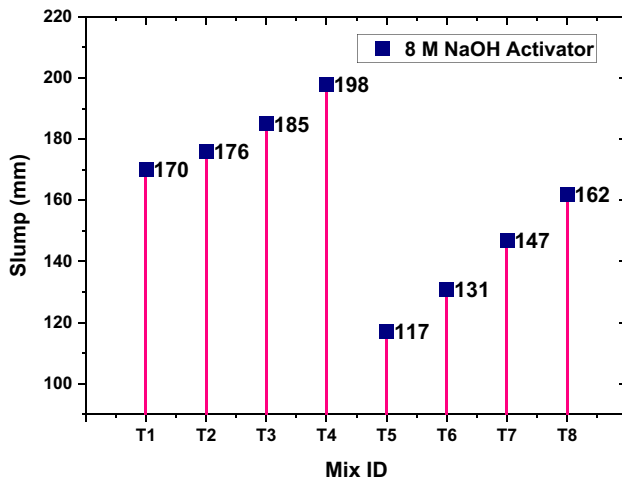


Fig. 3 Impact of WGP substitution levels on workability property

3 Results and Discussions

3.1 Workability Characteristics of Ternary Geopolymer Concrete

The effect of substitution levels of WGP (25–40 %) on the workability property of ternary geopolymer binder is depicted in Fig. 3. The slump cone test results illustrated in Fig. 3 stated that, an increase in the WGP replacement level increases the workability property of all the geopolymer mixes due to the less water absorption nature and smooth texture of WGP [29]. However, the maximum slump value of 198 mm is reported for the T4 mix constituting 50 % GGBS, 40 % WGP and 10 % MK. Due to the less reactive behavior of the silica content present in the MK, ternary geopolymer concrete blends encompassing 10 % MK (T1, T2, T3 & T4) exhibited superior workability results than mix proportions comprising 10 % FA (T5, T6, T7 & 8) in overall. From the other side, combinations containing 10 % FA achieved less workability results due to the highly reactive nature of the amorphous silica present in the FA.

3.2 Mechanical Characteristics of Ternary Geopolymer Concrete

The compressive strength development in the ternary-based geopolymer concrete mix proportions supplemented with different levels of WGP (25–40 %) in GGBS with 10 % of MK and FA activated using 8 M NaOH solution are represented in Fig. 4. According to Fig. 4, increasing the WGP substitution proportions (from 25 to 35 %) resulted in a gradual increase in the compressive strength of geopolymer samples containing 10 % MK (T1, T2, and T3). An increment in the compressive properties of geopolymer binder with an increase in WGP levels (25–35 %) is because of the

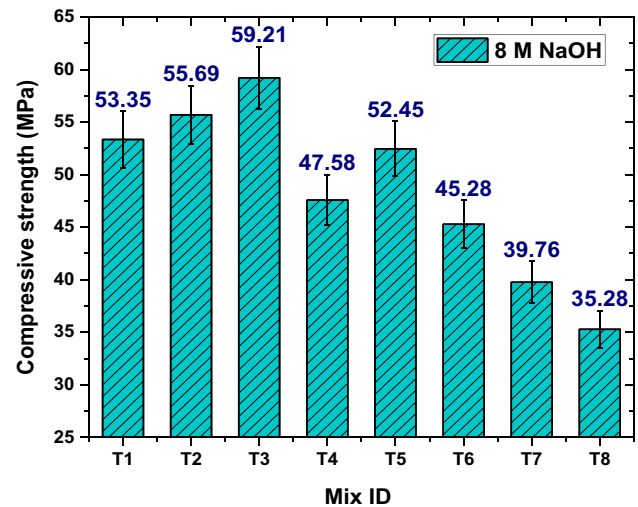


Fig. 4 Effect of WGP replacement levels on compressive strength

high reactive capability of SiO_2 proportion, which accelerates the geopolymerization reaction [8, 29, 34].

Further increment in the WGP replacement level of 40 % consequences in a noteworthy reduction in the compressive strength characteristics of T4 sample due to the development of low cross-linked aluminosilicate matrix on the increase in silica/alumina ratios [27, 35]. When WGP is introduced to ternary geopolymer samples containing 10 % FA (T5, T6, T7, and T8), the compressive strength gradually declines from 25 to 40 %. The inclusion of supplementary silica fraction into the geopolymer system via 10 % FA, which eventually increases the Silica/Alumina ratios, is the primary reason for the gradual decrease in compressive strength. For example, T5 geopolymer sample produced a maximum compressive strength of 52.45 MPa with a WGP replacement level of 25 % among the samples comprising 10 % FA. Out of all the proposed mix proportions, T3 reports the highest compressive strength value of 59.21 MPa with 50 % GGBS: 35 % WGP: 10 % MK.

Figure 5, illustrated the split-tensile behavior of the ternary blended geopolymer matrix comprising various substitution percentages of WGP for GGBS with a constant proportion of MK and Fly ash. As seen in Fig. 5, increasing the WGP levels (from 25 to 35 %) in geopolymer concrete samples constituting 10 % MK (T1, T2, and T3) resulted in a progressive increment in split-tensile strength. The improvement in the split-tensile behavior is attributed to the filling capability and pozzolanic nature of WGP, which strengthens the Interfacial Transition Zone (ITZ) between the binder and aggregates [10, 12].

The decrement in the split-tensile properties was observed for the 40 % WGP replacement level in the ternary mix due to the brittle characteristics of WGP [29]. Because of the development of high volume alkalis in the end products,

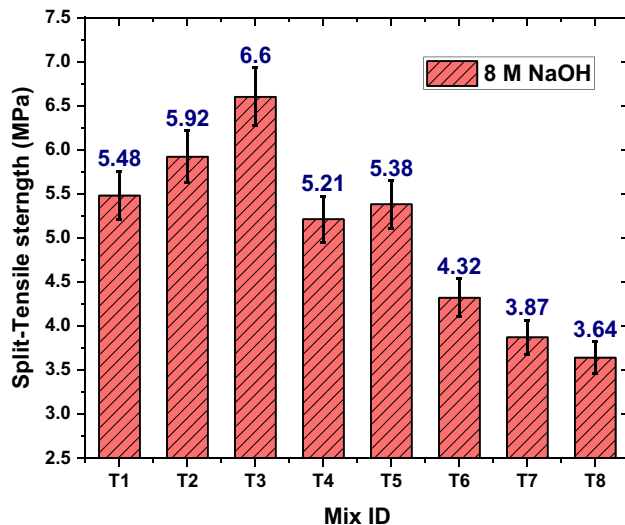


Fig. 5 Effect of WGP replacement levels on split-tensile strength

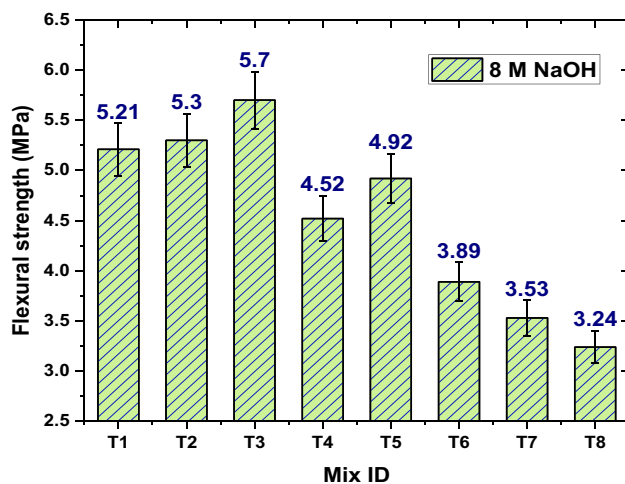


Fig. 6 Impact of WGP replacement percentages on flexural strength

the split-tensile results of geopolymer samples featuring 10 % FA (T5, T6, T7, and T8) decrease monotonically with increasing WGP replacement levels. The optimum substitution levels of WGP in ternary-based geopolymer concrete under the influence of split-tensile behavior for 10 % FA and 10 % MK were measured to be 25 % and 35 %, respectively.

The strength formation pattern observed from the three-point bending (flexure) test on the ternary blended geopolymer binder is similar to the split-tensile and compression test due to the proportions of the source materials employed in mix proportions. The flexural strength pattern of the ternary geopolymer matrix having different replacement percentages of WGP from (25–40 %) activated with 8 M NaOH solution is demonstrated in Fig. 6. T3 geopolymer mix comprising 35 % WGP, 55 % GGBS, and 10 % MK provided a maximum

flexural strength of 5.70 MPa under a three-point bending test. Similarly, among the geopolymer samples containing 10 % FA, the T5 sample has the highest flexural strength (4.92 MPa). Under flexural behavior, the optimal replacement levels of WGP in ternary geopolymer concrete for 10 % MK and FA were found to be 35 % and 25 %, respectively. Further increase in the WGP substitution percentages negatively impacts the flexural strength because of the lower reactive nature of parent materials present in the WGP than GGBS, MK and FA [36, 37].

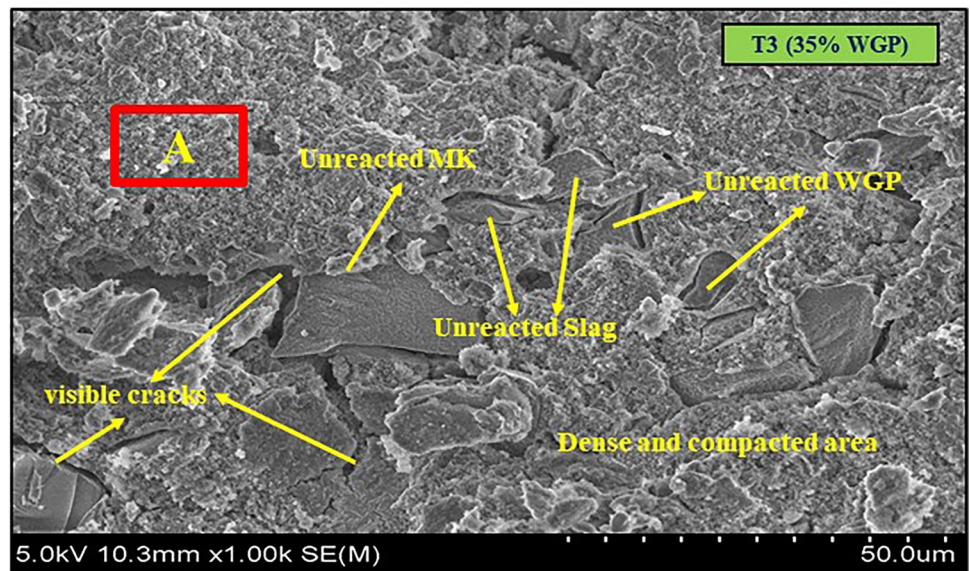
3.3 Mineralogical and Microstructural Characterization

Depending on the higher mechanical (compressive, split-tensile & flexural) strength values recorded in Section 3.2, geopolymer mix T3 constituting 55 % GGBS, 35 % WGP and 10 % MK is preferred for microstructural (SEM & EDX) and mineralogical (XRD) characterization. The SEM and EDX examination of the T3 geopolymer sample containing 55 % GGBS, 35 % WGP and 10 % MK activated using 8 M concentration of sodium hydroxide solution after 28 days of ambient curing environment is displayed in Fig. 7. As seen in Fig. 7(a) that a considerable amount of unreacted (or) partially activated WGP and GGBS particles exist because of the formation of semi-homogeneous gel [38]. The emergence of more visible/micro-cracks and less microstructure density occurs owing to the increment in WGP proportion, resulting in the generation of poor aluminosilicate cross-linked networks [35, 37].

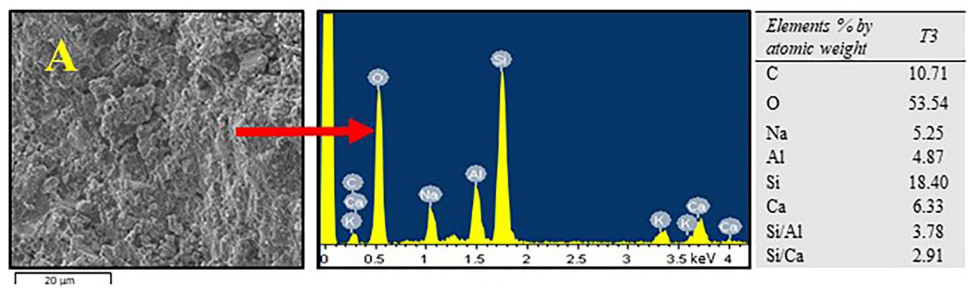
The EDX examination of the selected segment on the hardened geopolymer sample (T3) shown in Fig. 7(b) revealed substantial fractions of oxygen (O) & silica (Si) elements and small proportions of calcium (Ca) and sodium (Na) elements. The existence of these substances in the end product confirms the development of AL-O-SI bonds, sodium aluminate silicate hydrate (N-A-S-H) gels, and calcium aluminate silicate hydrate (C-A-S-H) gels during the geopolymer binder hardening phase [14, 39].

From EDX analysis, the silica/alumina and silica/calcium ratios of the T3 specimen constituting 35 % WGP: 55 % GGBS: 10 % MK are obtained as 3.78 and 2.91, respectively. According to earlier studies, the silica/alumina ratio (3.78) of the T3 sample is well within the recommended range of 3.5 - 4.0 for acceptable strength development, which entitle to arrive under the classification of a 3D network of polysialate-siloxo and poly-sialate-disiloxo polymer matrix [40, 41]. Furthermore, the silicon/alumina ratios of the geopolymer samples evaluated using EDX analysis increases as WGP substitution levels increase, which is consistent with the findings derived from mix design calculations (refer Table 3).

Fig. 7 SEM and EDX spectra of T3 geopolymer sample



(a)



(b)

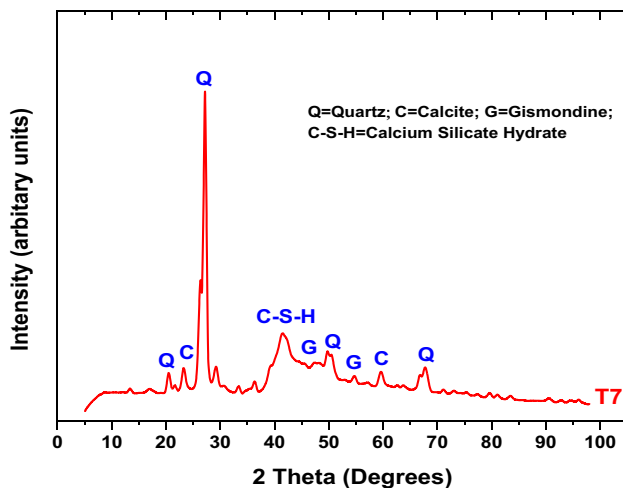


Fig. 8 X-ray diffractogram analysis of T3 geopolymer sample

Figure 8, displays the XRD diffractogram of T3 ternary geopolymer specimen activated with 8 M sodium hydroxide solution at the end of 28 days of ambient environment curing. The XRD pattern of T3 sample depicts the presence of Quartz (PDF # 00-046-1045), Calcite (PDF #

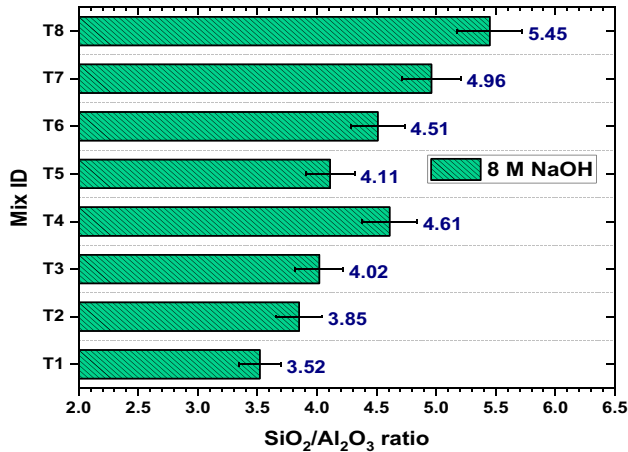
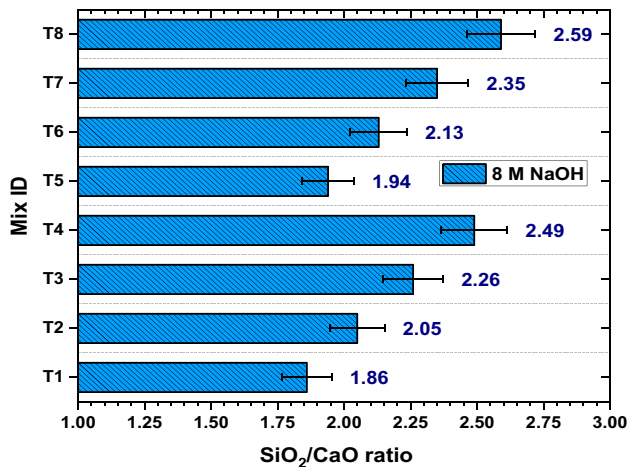
00-005-0586), calcium-based compound Gismondine (PDF # 04-01106245) and C-S-H gel. The existence of C-S-H gel is mainly responsible for the strength development in the geopolymer matrix designated by the rise in the peak levels ranging from 37° to 43° along (2θ) for the T3 sample. Furthermore, the generation of N-A-S-H gel is substantiated by the appearance of Gismondine peaks [37, 42]. The appearance of other peaks like Calcite and Quartz eventually enhances the mechanical strength characteristics of the geopolymer matrix by acting as filler material [34].

3.4 Influence of SiO₂/Al₂O₃ and SiO₂/CaO Fractions on Mechanical Properties of Geopolymers

Table 3 enumerates the aluminosilicate (binder) percentages and their respective ratios for different levels of WGP replacements (25–40%) utilized in ternary mixed geopolymers. The binder constituent fractions are determined primarily by the mix proportions and the chemical properties of the aluminosilicate source materials used in the study. The amount of CaO is controlled by raising the WGP levels as a GGBS substitute while keeping the steady percentage of MK/FA. Consequently, the proportions of SiO₂ and Al₂O₃

Table 3 Percentages of aluminosilicate sources and corresponding fractions

| Mix ID | Slag (%) | WGP (%) | MK (%) | FA (%) | SiO ₂ /Al ₂ O ₃ | SiO ₂ /CaO |
|--------|----------|---------|--------|--------|--|-----------------------|
| T1 | 65 | 25 | 10 | - | 3.52 | 1.86 |
| T2 | 60 | 30 | 10 | - | 3.85 | 2.05 |
| T3 | 55 | 35 | 10 | - | 4.02 | 2.26 |
| T4 | 50 | 40 | 10 | - | 4.61 | 2.49 |
| T5 | 65 | 25 | - | 10 | 4.11 | 1.94 |
| T6 | 60 | 30 | - | 10 | 4.51 | 2.13 |
| T7 | 55 | 35 | - | 10 | 4.96 | 2.35 |
| T8 | 50 | 40 | - | 10 | 5.45 | 2.59 |

**Fig. 9** Influence of SiO₂/Al₂O₃ ratios on the ternary geopolymer samples**Fig. 10** Influence of SiO₂/CaO ratios on the ternary geopolymer samples

are enhanced in the geopolymer system by incorporating WGP and MK/FA contents, respectively.

Figures 9 and 10, demonstrated the influence of different silica/alumina and silica/calcium fractions on the mechanical

characteristics of the ternary geopolymer samples. The SiO₂/Al₂O₃ ratio increases monotonically with the increment in the WGP percentage in the geopolymer matrix, as presented in Fig. 9. In the same way, gradually increasing WGP levels in a geopolymer system improves SiO₂/CaO ratios, as displayed in Fig. 10.

The maximum compressive (59.21 MPa) strength, split-tensile (6.60 MPa), and flexural strength (5.70 MPa) results are observed for T3 geopolymer mix containing SiO₂/Al₂O₃ and SiO₂/CaO ratios of 4.02 and 2.26, respectively. An increase in the silica/alumina and silica/calcium fractions enhances the formation of weaker aluminosilicate gels with reduced mechanical performance [35]. The optimum silica to alumina fraction values for achieving good strength characterization in geopolymer concrete suggested by various researches ranging from 3.5 to 4.0 [40]. Gradual increment of WGP proportions in the ternary blended geopolymer concrete results in increased SiO₂/Al₂O₃ and SiO₂/CaO ratios, reducing the molecular structure and mechanical strength characterizations [41].

4 Conclusions

The present study examined the changes in ternary blended geopolymer concrete's workability and mechanical properties based on the combination of GGBS, WGP with Metakaolin, and Fly ash. Based on the investigational findings, the subsequent outcomes could be framed:

- Grounded WGP can be utilized as a precursor raw ingredient in the preparation of a sustainable ternary geopolymer matrix.
- The increment in WGP replacement levels (from 25 to 40%) improved the workability characteristics of the fresh geopolymer matrix for all eight mix proportions due to its lower water absorption ability and smooth surface area.
- The fraction of 55% GGBS, 35% WGP, 10% MK with 8 M NaOH solution furnished highest compressive (59.21 MPa) strength, split-tensile (6.60 MPa) and flexural strength (5.70 MPa) results respectively.

- XRD and microstructural (SEM & EDX) examinations of the geopolymer sample (T3) reported the existence of AL-O-SI, C-A-S-H, and N-A-S-H formations as reaction outcomes during the geopolymerization processes.
- The mechanical properties (compressive strength, split-tensile strength, and flexural strength) of the ternary geopolymer matrix are reduced as the $\text{SiO}_2/\text{Al}_2\text{O}_3$ and SiO_2/CaO ratios increase with the consequent increase of WGP substitution levels.
- This suggested research work could open the direction for the progression of the sustainable ternary geopolymer binder under ambient curing environments using WGP, enabling the replacement of traditional cement-based concrete in practical applications such as sewer pipelines, spillways, crash barriers, railway sleepers, precast elements, shotcrete, road construction, repair materials, pile caps, manholes, and so on.

Acknowledgements The authors would like to express their gratitude to the Vellore Institute of Technology in Chennai, India, for their generous support and motivation in carrying out this research. The authors wish to thank the Fosroc Chemicals India Private Limited, Chennai and the Regional Concrete Manager Er. S. Duraimurugan for his support and the facilities rendered to carry out this research work.

Credit Authorship Contribution P. Manikandan: Methodology, Validation, Formal analysis, Investigation, Writing original draft, Writing – review & editing, Visualization. L. Natrayan: Formal analysis, Writing – review & editing. S. Duraimurugan: Resources, Supervision, Funding acquisition, Writing – review & editing. V. Vasugi: Conceptualization, Writing – review and editing, Visualization, Supervision.

Funding The work was supported by the Fosroc Chemicals India Private Limited, Chennai. Grant number KMB/96ANC-12/2019.

Data Availability The data sources used in this research are accessible upon proper request from the corresponding author.

Declarations

There are no investigations with human participants or animals practiced by any of the authors in this article.

Declaration of Competing Interest The authors proclaim that they have no known competing financial interests or personal relationships that could have influenced the research presented in this paper.

Consent to Participate Not applicable.

Consent for Publication Not applicable.

References

1. Bheel N, Adesina A (2020) Influence of binary blend of corn cob ash and glass powder as partial replacement of cement in concrete. *Silicon*. <https://doi.org/10.1007/s12633-020-00557-4>
2. Jan A, Pu Z, Khan KA, et al (2021) A review on the effect of silica to alumina ratio, alkaline solution to binder ratio, calcium oxide + ferric oxide. Molar concentration of sodium hydroxide and sodium silicate to sodium hydroxide ratio on the compressive strength of geopolymer concrete. *Silicon*. <https://doi.org/10.1007/s12633-021-01130-3>
3. Mustakim SM, Das SK, Mishra J, et al (2020) Improvement in fresh, mechanical and microstructural properties of fly ash- blast furnace slag based geopolymer concrete by addition of nano and micro silica. *Silicon*. <https://doi.org/10.1007/s12633-020-00593-0>
4. Manikanta C, Manikandan P, Duraimurugan S, et al (2020) Pozzolanic properties of agro waste ashes for potential cement replacement predicted using ANN. *J Phys Conf Ser*, p 012018
5. Provis JL (2014) Green concrete or red herring? - Future of alkali-activated materials. *Adv Appl Ceram* 113:472–477. <https://doi.org/10.1179/1743676114Y.0000000177>
6. He P, Zhang B, Yang S et al (2020) Recycling of glass cullet and glass powder in alkali-activated cement: mechanical properties and alkali-silica reaction. *Waste Biomass Valorization* 11:7159–7169. <https://doi.org/10.1007/s12649-020-01102-5>
7. Chaitanya M, Manikandan P, Prem Kumar V, et al (2020) Prediction of self-healing characteristics of GGBS admixed concrete using artificial neural network. *J Phys Conf Ser*, p 012019
8. Aliabdo AA, Abd Elmoaty AEM, Aboshama AY (2016) Utilization of waste glass powder in the production of cement and concrete. *Constr Build Mater* 124:866–877. <https://doi.org/10.1016/j.conbuildmat.2016.08.016>
9. Kou SC, Poon CS (2009) Properties of self-compacting concrete prepared with recycled glass aggregate. *Cem Concr Compos* 31:107–113. <https://doi.org/10.1016/j.cemconcomp.2008.12.002>
10. Mallum I, Abdul AR, Lim NHAS, Omolayo N (2021) Sustainable utilization of waste glass in concrete: a review. *Silicon*. <https://doi.org/10.1007/s12633-021-01152-x>
11. Lu J, xin, Duan Z hua, Poon CS. (2017) Combined use of waste glass powder and cullet in architectural mortar. *Cem Concr Compos* 82:34–44. <https://doi.org/10.1016/j.cemconcomp.2017.05.011>
12. Manikandan P, Vasugi V (2021) A critical review of waste glass powder as an aluminosilicate source material for sustainable geopolymer concrete production. *Silicon* 13:3649–3663. <https://doi.org/10.1007/s12633-020-00929-w>
13. Ling TC, Poon CS (2017) Spent fluorescent lamp glass as a substitute for fine aggregate in cement mortar. *J Clean Prod* 161:646–654. <https://doi.org/10.1016/j.jclepro.2017.05.173>
14. Davidovits J (1991) Geopolymers. *J Therm Anal* 37:1633–1656. <https://doi.org/10.1007/bf01912193>
15. Rajamane NP, Nataraja MC, Jeyalakshmi R, Nithiyanantham S (2015) Greener durable concretes through geopolymerisation of blast furnace slag. *Mater Res Express* 2:1–8. <https://doi.org/10.1088/2053-1591/2/5/055502>
16. Nagajothi S, Elavenil S (2021) Effect of GGBS addition on reactivity and microstructure properties of ambient cured fly ash based geopolymer concrete. *Silicon* 13:507–516. <https://doi.org/10.1007/s12633-020-00470-w>
17. Jithendra C, Elavenil S (2020) Effects of silica fume on workability and compressive strength properties of aluminosilicate based flowable geopolymer mortar under ambient curing. *Silicon* 12:1965–1974. <https://doi.org/10.1007/s12633-019-00308-0>
18. Parathi S, Nagarajan P, Pallikkara SA (2021) Ecofriendly geopolymer concrete: a comprehensive review. *Clean Technol Environ Policy*. <https://doi.org/10.1007/s10098-021-02085-0>
19. AbdulAleem MI, Arumairaj PD (2011) A review of seismic assessment of reinforced concrete structure using pushover analysis. *Int J Eng Sci Emerg Technol* 1:118–122
20. Hassan A, Arif M, Shariq M (2019) Use of geopolymer concrete for a cleaner and sustainable environment – A review of

- mechanical properties and microstructure. *J Clean Prod* 223:704–728. <https://doi.org/10.1016/j.jclepro.2019.03.051>
21. Mo KH, Alengaram UJ, Jumaat MZ (2016) Structural performance of reinforced geopolymer concrete members: A review. *Constr Build Mater* 120:251–264. <https://doi.org/10.1016/j.conbuildmat.2016.05.088>
 22. Magesh M, Jawahar S, Dhanesh E, Vasugi V (2019) Influence of bottom ash as fine aggregate in ggbs geopolymer concrete. *Int J Innov Technol Explor Eng* 8:919–924
 23. Rahman A, Barai A, Sarker A, Moniruzzaman M (2018) Light weight concrete from rice husk ash and glass powder. *Bangladesh J Sci Ind Res* 53:225–232. <https://doi.org/10.3329/bjsir.v53i3.38270>
 24. Okoye FN, Durgaprasad J, Singh NB (2016) Effect of silica fume on the mechanical properties of fly ash based-geopolymer concrete. *Ceram Int* 42:3000–3006. <https://doi.org/10.1016/j.ceramint.2015.10.084>
 25. Duan P, Yan C, Zhou W, Luo W (2016) Fresh properties, mechanical strength and microstructure of fly ash geopolymer paste reinforced with sawdust. *Constr Build Mater* 111:600–610. <https://doi.org/10.1016/j.conbuildmat.2016.02.091>
 26. Wongsu A, Boonserm K, Waisurasingha C, et al (2017) Use of municipal solid waste incinerator (MSWI) bottom ash in high calcium fly ash geopolymer matrix. *J Clean Prod* 148:49–59. <https://doi.org/10.1016/j.jclepro.2017.01.147>
 27. Torres-Carrasco M, Puertas F (2015) Waste glass in the geopolymer preparation. Mechanical and microstructural characterisation. *J Clean Prod* 90:397–408. <https://doi.org/10.1016/j.jclepro.2014.11.074>
 28. Kumar P, Pankar C, Manish D, Santhi AS (2018) Study of mechanical and microstructural properties of geopolymer concrete with GGBS and Metakaolin. *Mater Today Proc* 5:28127–28135. <https://doi.org/10.1016/j.matpr.2018.10.054>
 29. Mehta A, Ashish DK (2020) Silica fume and waste glass in cement concrete production: A review. *J Build Eng* 29:100888. <https://doi.org/10.1016/j.jobbe.2019.100888>
 30. Ma CK, Awang AZ, Omar W (2018) Structural and material performance of geopolymer concrete: A review. *Constr Build Mater* 186:90–102. <https://doi.org/10.1016/j.conbuildmat.2018.07.111>
 31. BIS:383-1970 (1970) Specification for coarse and fine aggregates from natural sources for concrete. *Bur Indian Stand*, New Delhi, India, pp 1–24
 32. BIS:7320-1974 (1974) Specifications for concrete slump test apparatus. *Bur Indian Stand* New Delhi, India 1–14
 33. IS 516:2014 (2004) Method of tests for strength of concrete. IS 516 - 1959 (Reaffirmed 2004) New Delhi, India
 34. Burciaga-Díaz O, Durón-Sifuentes M, Díaz-Guillén JA, Escalante-García JI (2020) Effect of waste glass incorporation on the properties of geopolymers formulated with low purity metakaolin. *Cem Concr Compos* 107. <https://doi.org/10.1016/j.cemconcomp.2019.103492>
 35. Tho-In T, Sata V, Boonserm K, Chindaprasirt P (2016) Compressive strength and microstructure analysis of geopolymer paste using waste glass powder and fly ash. *J Clean Prod* 172:2892–2898. <https://doi.org/10.1016/j.jclepro.2017.11.125>
 36. Shoaei P, Ameri F, Reza Musaei H, et al (2020) Glass powder as a partial precursor in Portland cement and alkali-activated slag mortar: A comprehensive comparative study. *Constr Build Mater* 251:118991. <https://doi.org/10.1016/j.conbuildmat.2020.118991>
 37. Khan MNN, Kuri JC, Sarker PK (2021) Effect of waste glass powder as a partial precursor in ambient cured alkali activated fly ash and fly ash-GGBFS mortars. *J Build Eng* 34:101934. <https://doi.org/10.1016/j.jobbe.2020.101934>
 38. Zhang S, Keulen A, Arbi K, Ye G (2017) Waste glass as partial mineral precursor in alkali-activated slag/fly ash system. *Cem Concr Res* 102:29–40. <https://doi.org/10.1016/j.cemconres.2017.08.012>
 39. Ganesh AC, Muthukannan M (2021) Development of high performance sustainable optimized fiber reinforced geopolymer concrete and prediction of compressive strength. *J Clean Prod* 282:124543. <https://doi.org/10.1016/j.jclepro.2020.124543>
 40. Chindaprasirt P, Rattanasak U, Vongvoradit P, Jenjirapanya S (2012) Thermal treatment and utilization of Al-rich waste in high calcium fly ash geopolymeric materials. *Int J Miner Metall Mater* 19:872–878. <https://doi.org/10.1007/s12613-012-0641-z>
 41. Silva P De, Sagoe-Crenstil K, Sirivivatnanon V (2007) Kinetics of geopolymerization: Role of Al₂O₃ and SiO₂. *Cem Concr Res* 37:512–518. <https://doi.org/10.1016/j.cemconres.2007.01.003>
 42. Fletcher RA, MacKenzie KJD, Nicholson CL, Shimada S (2005) The composition range of aluminosilicate geopolymers. *J Eur Ceram Soc* 25:1471–1477. <https://doi.org/10.1016/j.jeurceramsoc.2004.06.001>

Publisher's Note Springer Nature remains neutral with regard to jurisdictional claims in published maps and institutional affiliations.